Vorinostat, a pan-HDAC inhibitor, abrogates productive HPV-18 DNA amplification

N. Sanjib Banerjee[a,1], Dianne W. Moore[a], Thomas R. Broker[a], and Louise T. Chow[a,1]

[a]Department of Biochemistry and Molecular Genetics, University of Alabama at Birmingham, Birmingham, AL 35294-0005

Contributed by Louise T. Chow, September 24, 2018 (sent for review January 22, 2018; reviewed by Richard B. Roden and Renske D. M. Steenbergen)

Human papillomaviruses (HPVs) cause epithelial proliferative diseases. Persistent infection of the mucosal epithelia by the high-risk genotypes can progress to high-grade dysplasia and cancers. Viral transcription and protein activities are intimately linked to regulation by histone acetyltransferases and histone deacetylases (HDACs) that remodel chromatin and regulate gene expression. HDACs are also essential to remodel and repair replicating chromatin to enable the progression of replication forks. As such, Vorinostat (suberoylanilide hydroximic acid), and other pan-HDAC inhibitors, are used to treat lymphomas. Here, we investigated the effects of Vorinostat on productive infection of the high-risk HPV-18 in organotypic cultures of primary human keratinocytes. HPV DNA amplifies in the postmitotic, differentiated cells of squamous epithelia, in which the viral oncoproteins E7 and E6 establish a permissive milieu by destabilizing major tumor suppressors, the pRB family proteins and p53, respectively. We showed that Vorinostat significantly reduced these E6 and E7 activities, abrogated viral DNA amplification, and inhibited host DNA replication. The E7-induced DNA damage response, which is critical for both events, was also compromised. Consequently, Vorinostat exposure led to DNA damage and triggered apoptosis in HPV-infected, differentiated cells, whereas uninfected tissues were spared. Apoptosis was attributed to highly elevated proapoptotic Bim isoforms that are known to be repressed by EZH2 in a repressor complex containing HDACs. Two other HDAC inhibitors, Belinostat and Panobinostat, also inhibited viral DNA amplification and cause apoptosis. We suggest that HDAC inhibitors are promising therapeutic agents to treat benign HPV infections, abrogate progeny virus production, and hence interrupt transmission.

HPV DNA amplification | HDAC inhibitors | organotypic cultures | HPV E6 and E7 activities | apoptosis

The prevalent human papillomaviruses infect the basal cells of mucosal or cutaneous squamous epithelia, causing hyperproliferative lesions. The low-risk (LR) mucosotropic HPVs cause 90% of anogenital warts and all laryngeal papillomas, whereas persistent infection by the high-risk (HR) virus types can progress to carcinomas, including anogenital and head and neck cancers (1). The virus gains entry into the basal cells of a squamous epithelium through a wound. In benign lesions, viral activities are low in the basal cells, and the productive program depends on squamous differentiation, which occurs in the middle and upper strata. Following DNA amplification, capsid proteins are synthesized and progeny virus particles are assembled in the uppermost strata and shed with the desquamated cells (2). Our laboratory has recapitulated a robust productive program of HR HPV-18 in organotypic raft cultures of primary human keratinocytes (PHKs) (3). To support viral production in postmitotic, differentiated keratinocytes, HPVs express E7 and E6 proteins to target pRB family pocket proteins and p53, respectively (4). The p130 pocket protein maintains the homeostasis of differentiated cells. The HR and LR E7 proteins mediate p130 destabilization, thereby reactivating cell cycle genes to promote S-phase reentry (5). E7 also induces the DNA damage response (DDR), which safeguards proper cellular DNA replication and is required to support viral DNA amplification (6–8). Importantly, DDR prolongs G2 phase, during which the host replication machinery becomes available to support virus DNA amplification (3, 7). The DDR kinases also phosphorylate and stabilize p53 protein (9). Among its diverse functions (10), E6-mediated destabilization of p53 is necessary to permit high levels of HPV DNA amplification (3, 11).

Histone acetyltransferases (HATs) add acetyl groups to lysine residues in histones and nonhistone regulatory proteins, whereas histone deacetylases (HDACs) remove them. The former modifications result in an open chromatin structure to activate RNA transcription, whereas the latter lead to a compact chromatin to inhibit transcription (12). Eighteen mammalian HDACs have been broadly grouped into four classes (13). Briefly, in addition to acting on histones, class I (HDAC-1, HDAC-2, and HDAC-3), class IIa [HDAC-4 and -5, class IIb (HDAC-6)], and class III (Sirtuin-1, Sirtuin-2, Sirtuin-3, Sirtuin-5, Sirtuin-6, and Sirtuin-7) are components of repressor complexes that regulate growth, development, cell migration, apoptosis, and DNA damage repair (13–16).

HPV infections establish extensive interactions with HATs and HDACs. HATs and HDACs can regulate transcription of the E6 and E7 genes from the promoter located in upstream regulatory region (URR; i.e., long control region). HDAC-1 recruits SMAR1 to the HPV-18 URR to down-regulate cFos-dependent transcription in HeLa cells (17). Trichostatin A (TSA), a pan-HDAC inhibitor, derepresses the HPV URR-driven LacZ reporter in the basal stratum of PHK raft cultures (18). Tip60 acetylates histone H4 and recruits Brd4, resulting in repression of the HPV URR promoter in the presence or absence of the viral E2 protein in transformed epithelial cell lines (19, 20). To counter this repression, LR and HR HPV E6 proteins destabilize Tip60 to

Significance

Persistent infection by the high-risk human papillomaviruses (HPVs) can lead to anogenital and head and neck cancers. The HPV vaccines effectively prevent new type-restricted infections but have no effect on preexisting infections. It is crucial to identify effective inhibitors of preneoplastic HPV infections. Histone deacetylases (HDACs) modulate chromatin structure and transcription, and are also essential for chromatin replication fork progression. Here we show that Vorinostat, a pan-HDAC inhibitor, stabilizes host cell tumor suppressors targeted by HPV oncoproteins E6 and E7 and abrogates productive infection by a high-risk HPV in organotypic cultures of human keratinocytes. Furthermore, Vorinostat selectively induces apoptosis in HPV-infected cells by decreasing DNA repair response while increasing the proapoptotic protein Bim. Vorinostat appears to be a promising therapeutic agent.

Author contributions: N.S.B. and L.T.C. designed research; N.S.B. and D.W.M. performed research; N.S.B., T.R.B., and L.T.C. analyzed data; and N.S.B., T.R.B., and L.T.C. wrote the paper.

Reviewers: R.B.R., Johns Hopkins University; and R.D.M.S., Amsterdam UMC.

The authors declare no conflict of interest.

[1]To whom correspondence may be addressed. Email: banerjee@uab.edu or ltchow@uab.edu.

This article contains supporting information online at www.pnas.org/lookup/suppl/doi:10.1073/pnas.1801156115/-/DCSupplemental.

Published online November 1, 2018.

derepress the URR promoter as well as promoters of certain cellular genes. In particular, destabilization of Tip60 abrogates p53-dependent apoptosis (20). Furthermore, E6 can inactivate the transacting function of p53 by inhibiting p300-mediated acetylation of p53 and nucleosome core histones (21). Thus, in certain transformed cell lines, HDAC inhibitors increase acetylation, leading to elevated p53 activity and increased p53-stimulated expression of proapoptotic proteins such as Apaf1, Puma, and Noxa (9). E7 destabilizes the pRB family pocket proteins that normally recruit HDACs to inhibit cell cycle genes (22). Moreover, HPV-31 E7 binds and inhibits HDACs, thereby facilitating virus replication through activation of E2F2 transcription (23). SirT1, which inactivates pRB pocket proteins (24) and p53 (25, 26), is induced by HPV-16 E7 (27, 28) and by HPV-31 E6 and E7 (29). SirT1 associates with the HPV genome and participates in chromatin remodeling and in recruitment of homologous DNA repair proteins necessary for viral genome maintenance and replication (29). However, in the absence of HPV oncoproteins, SirT1 inhibits the transient replication of HPV-16 origin-containing plasmid by deacetylation of the HPV E2 protein in the C33a cell line, an HPV-negative cervical cancer cell line (30).

In addition to regulating gene expression, class I HDACs also remodel replicating chromatin, an activity which is essential for fork progression during chromatin replication and damage repair for in vivo viability and development (31). Indeed, Vorinostat and other pan-HDAC inhibitors of class I, IIa, IIb, and IV HDACs effectively inhibit growth of cancer cell lines and patient-derived xenografts. Consequently, HDAC inhibitors have emerged as chemotherapeutic agents alone or in combination with other anticancer agents to treat multiple myeloma and lymphoma (32). HDACs are also elevated in cervical dysplasia and cancers relative to the normal epithelium, and TSA or Vorinostat in combination with the proteasome inhibitor bortezomib is lethal against cervical cancer cell lines in vitro or in nude mice xenografts (33). However, the mechanisms were not investigated.

Because of the demonstrated intricate interactions among HPVs, HATs, and HDACs, the E7-induced S-phase reentry in the differentiated strata and, in particular, the critical role of HDACs in chromatin remodeling during DNA replication, we hypothesized that a pan-HDAC inhibitor would also adversely affect viral DNA amplification. First, an HDAC inhibitor would prevent S-phase progression to G2 in suprabasal cells in which viral DNA amplification occurs. Second, replicating forks of chromatinized viral DNA would also stall, possibly resulting in its loss to degradation. Third, the arrest of host chromatin fork progression could lead to DNA damage and apoptosis, as it does in cancer cells. We tested this hypothesis in the productively infected HPV-18 model system. The results indeed revealed Vorinostat to be an effective inhibitor of HPV-18 DNA amplification and induced apoptosis in a fraction of differentiated cells. In contrast, uninfected PHK raft cultures were largely spared. We also examined the effects of Vorinostat on levels and functions of viral oncoproteins and elucidated the mechanisms that led to apoptosis in HPV-18–infected cultures. Finally, we showed that raft cultures of an HPV-16 immortalized cell line and HPV-16 transformed cervical cancer cells were highly sensitive to Vorinostat, leading to tissue death.

Materials and Methods

Replicative HPV-18 plasmid was generated via in vivo recombination in early passage (P0 or P1) PHKs transfected with recombinant DNA plasmids (3). Independent experiments used different batches of PHKs. In each set of experiments, raft cultures were prepared from the same batch of untransfected PHKs and from HPV-18 containing (hereinafter indicated as infected) PHKs. They were untreated (UT) or exposed to vehicle (0.1% DMSO), Vorinostat, Belinostat, or Panobinostat as detailed in *Results*. BrdU was added to culture medium for 6 h before harvest to mark S-phase cells. Multiplicative raft cultures were harvested either frozen for protein and DNA analysis or formalin-fixed and paraffin-embedded (FFPE) for in situ studies. Additional information can be found in *SI Appendix*.

Results

Effects on Tissue Histology. We conducted multiple independent experiments in which the control PHK and HPV-18 raft cultures were exposed to DMSO vehicle (final concentration of 0.1%) or increasing concentrations of Vorinostat (SAHA) from day 6 to day 13. Histology of day 13 cultures was analyzed after H&E staining. At 0.2 μM, Vorinostat had no discernable effect on either culture (*SI Appendix*, Fig. S1). At 5 μM, Vorinostat induced hypertrophy (enlarged cells) in the infected cultures. Additional morphological features of cytotoxicity such as vacuolated cells or cells with condensed nuclei were observed in the suprabasal layers, much more so in HPV-18–infected cultures than in PHK cultures (Fig. 1). In 1 μM-treated PHK raft cultures, hypertrophy was already evident, and formation of stratum granulosum was inhibited (Fig. 1*B*). The expression of late differentiation marker Loricrin, a component of granules in granulocytes, and early differentiation marker K10, normally present in all suprabasal cells, was more significantly and adversely impacted in

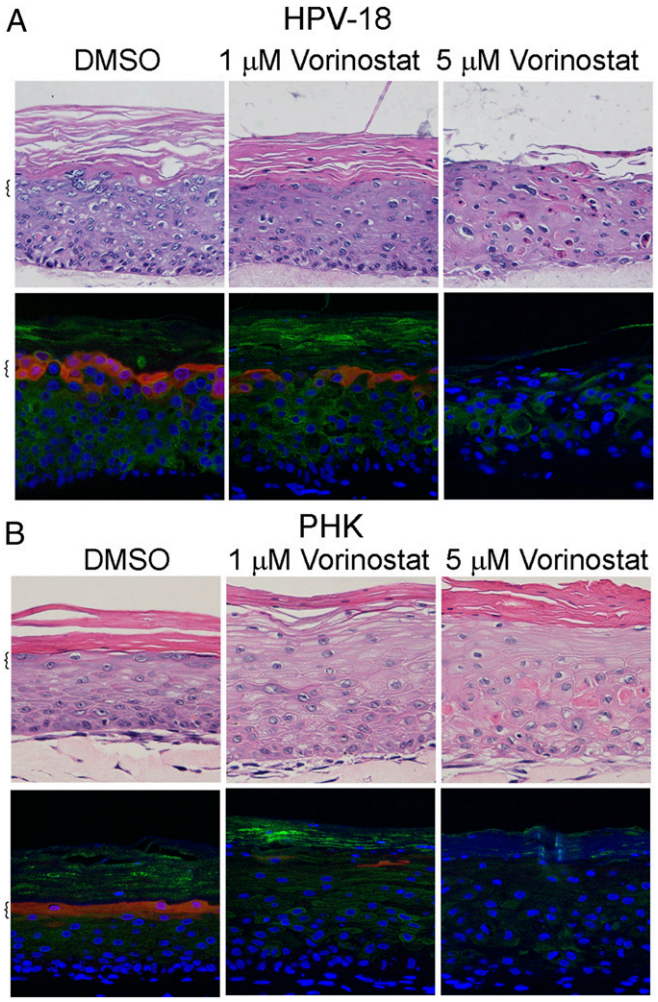

Fig. 1. Histology and differentiation markers of representative raft cultures. HPV-18 (*A*) infected and (*B*) uninfected day 13 PHK raft cultures were exposed, from days 6 to 13, to DMSO and 1 or 5 μM Vorinostat. Four-micrometer sections of FFPE tissues were stained with hematoxylin and eosin (*Upper*). Indirect IF detection of loricrin (red) and keratin 10 (green) (*Lower*). Brackets denote stratum granulosum. Microphotographic images here and in later figures were captured with a 20× objective, and DAPI staining (blue) revealed all nuclei.

uninfected cultures than in infected cultures (compare Fig. 1 *A* and *B*).

Inhibition of HPV-18 DNA Amplification and Major Capsid Protein Synthesis. Using quantitative real-time PCR, the effects of Vorinostat on the amplification of HPV-18 DNA were determined relative to vehicle-treated control raft cultures. In one set of experiments, the relative HPV-18 DNA copy number/cell did not decrease significantly in cultures exposed to 0.2 μM Vorinostat relative to the control culture. However, it was reduced by 94.0% or 98.7% in cultures treated with 5 or 10 μM Vorinostat, respectively (Fig. 2*A*). In another set of independent experiments, exposures to 2, 3, 4, or 5 μM Vorinostat reduced HPV-18 DNA copy numbers in a concentration-dependent manner (Fig. 2*B*). In subsequent experiments, we settled on using 0.2, 1, and 5 μM Vorinostat. As a negative control, we used UT or 0.1% DMSO vehicle (0 for no Vorinostat)-exposed PHK raft cultures and HPV-18–infected raft cultures.

Viral DNA fluorescence in situ hybridization (DNA-FISH) performed on slides from one of several sets of experiments confirmed the trend of reduction in viral DNA amplification in the presence of increasing Vorinostat concentrations (Fig. 2*C*). Quantitative analyses of images from four microscopic fields (at 20×) from each slide showed that, relative to the vehicle-treated control, the number of nuclei with HPV-18 DNA signals was reduced by 79% when exposed to 1 μM Vorinostat and by nearly 100% in 5 μM Vorinostat (Fig. 2*D*, orange bars). In addition, the pixel intensity of HPV-18 DNA signal per microscopic field was reduced from an average of 8,300 (±1,300) in the vehicle-treated control to 1,500 (±840) in 1 μM Vorinostat-treated cultures (Fig. 2*E*).

Indirect immunofluorescence (IF) detection of the major L1 capsid protein in DMSO carrier-treated HPV-18 cultures revealed copious signals in desquamated cellular envelopes above the live epithelium. The signals were greatly reduced or entirely abrogated in cultures exposed to 1 or 5 μg/mL of Vorinostat, respectively (Fig. 2*F*). These results are consistent with our understanding that viral capsid protein synthesis depends on viral DNA amplification (3, 11). Thus, we conclude that Vorinostat has prevented progeny virus production.

Inhibition of S-Phase Entry or Progression. HPV E7 protein promotes differentiated cells to reenter S phase in a stochastic manner (34). In the raft cultures, nascent cellular DNA replication was labeled by incorporation of the thymidine analog BrdU added to the culture medium for 6 h immediately before harvest. To examine the effect of Vorinostat on cellular DNA replication, we simultaneously probed for BrdU incorporation in the same sections used to detect viral DNA amplification by DNA-FISH (Fig. 2*C*). As shown previously (3), in vehicle-treated HPV-18 raft cultures, cellular DNA replication and HPV DNA amplification were temporally separated such that BrdU incorporation and amplified viral DNA were primarily detected in different nuclei. BrdU-positive cells were reduced in cultures treated with 1 μM Vorinostat for 7 d in HPV-18–infected cultures relative to vehicle-treated cultures. Hardly any signals were detected upon exposure to Vorinostat at 5 μM. These results were verified in multiple experiments. Quantitative analyses of four microscopic fields confirmed the reduction of BrdU-positive nuclei by 63% or 94% relative to the control cultures following exposures to 1 or 5 μM Vorinostat in the representative experimental set (Fig. 2*D*, blue bars).

We also probed for the effect of Vorinostat on host DNA replication in raft cultures of uninfected PHKs. In vehicle-exposed cultures, BrdU incorporation was stochastically detected exclusively in the basal stratum. The signals were reduced at 1 μM of Vorinostat and abrogated at 5 μM (Fig. 2*G*). Thus, the inhibitory effect of Vorinostat on host DNA replication appears to be similar in both normal and HPV-18 raft cultures.

Elevation of Histone 4 Acetylation and Modulation of HPV-Induced HDACs. To ensure that Vorinostat indeed inhibits the deacetylation of histones at the concentrations used in our experiments, we examined its effect on the levels of acetylated H4 as a representative target. In two independent experiments, in which HPV-18 DNA amplified to different levels (lysates designated a and b), immunoblots (IB) showed that antibodies to acetylated H4K5/K9/K12/K16 or H4K12 detected elevated signals in the HPV-18 raft culture treated with 5 μM Vorinostat (Fig. 3 *A* and *B*). Indirect IF assays of tissue sections revealed a large number of differentiated cells positive for H4K12Ac or for H4K16Ac. In contrast, the vehicle-treated cultures had very weak signals and only in a few cells (Fig. 3 *C* and *D*). Although the impact on viral and host DNA replication was evident at 1 μg/mL Vorinostat, we did not detect acetylated H4 by IF or IB, possibly due to the sensitivity of the antibody. For instance, at 2 μg/mL, indirect IF revealed widespread signals (Fig. 3*E*). These results verify the activity of Vorinostat. It is likely that H3 is similarly affected by the pan-HDAC inhibitor.

Because of the suprabasal S-phase reentry in infected cultures, we anticipated that certain HDACs would be elevated relative to uninfected cultures to meet the need for remodeling the replicating chromatin. To confirm this hypothesis, we probed IBs for various HDACs. HDAC-1, HDAC-3, HDAC-4, HDAC-5, and HDAC-6 were low in PHK raft cultures but were elevated upon HPV-18 infection (Fig. 4). HDAC-2 was high in uninfected cultures, and the increase in HPV-18–infected PHKs was relatively small. Interestingly, 5 μM Vorinostat, which abrogated host DNA replication, reduced HDAC-3, HDAC-4, HDAC-5, and HDAC-6, but not HDAC-1 and HDAC-2 (Fig. 4). The HDAC-7 signals were low in PHK raft cultures, and their modulation in response to HPV infection and by the subsequent Vorinostat exposure was relatively minor (Fig. 4*B*). As reported previously (29), we also observed slightly elevated SirT-1 in the HPV-infected cultures. This elevation was abrogated by 5 μM Vorinostat (Fig. 4*B*).

Reduction of E7 and E6 Activities. We found that, relative to vehicle-treated control, the E7 protein levels in HPV-18 raft cultures were not significantly altered at 0.2 and 1 μM in two independent experiments but were slightly reduced at 5 μM (Fig. 5*A*). As described previously, p130 was high in uninfected raft cultures and its level was greatly reduced in HPV-18–infected cultures and in cultures expressing E7 (3, 5). In cultures treated with Vorinostat, the levels of hypophosphorylated p130 pocket protein were elevated relative to UT HPV-18 cultures (Fig. 5*A*), consistent with diminished E7 activity. The stabilization of p130 could reduce S-phase reentry (5). Indeed, the E7 responsive protein, the proliferating cells nuclear antigen (PCNA), was detected only in a few cells, whereas the cyclin B1 were no longer detectible (Fig. 5*G*). The pRB protein level was also reduced in HPV-18–infected cultures relative to the uninfected PHK raft cultures. However, unlike p130, it was diminished at 5 μM of Vorinostat (Fig. 5*B*). The significance of this latter observation will be presented in *Discussion*.

HPV E7 activates E2F-responsive genes, thereby promoting S-phase reentry as well as DDR kinases that safeguard accurate chromosomal duplication (35). Some of these kinases in turn phosphorylate and stabilize p53 (36). The HR HPV E6 protein, in conjunction with the E3 ubiquitin ligase E6AP, binds and destabilizes p53 (37) to permit HPV DNA amplification (3, 11). IBs showed that steady-state levels of E6 were reduced in cultures exposed to 5 μM Vorinostat (Fig. 5*A*). Relative to uninfected raft cultures, p53 in HPV-18 raft cultures was much reduced, whereas its levels increased in cultures treated with 1 or 5 μM Vorinostat (Fig. 5*B*). These results suggest that the ability of E6 to destabilize p53 was adversely affected by Vorinostat. Intriguingly, the steady-state levels of E6AP were not altered in the presence or absence of HPV-18 infection, nor upon exposures to Vorinostat (Fig. 5*C*). This result is unlike the report of E6-induced E6AP degradation in submerged cancer cells (38),

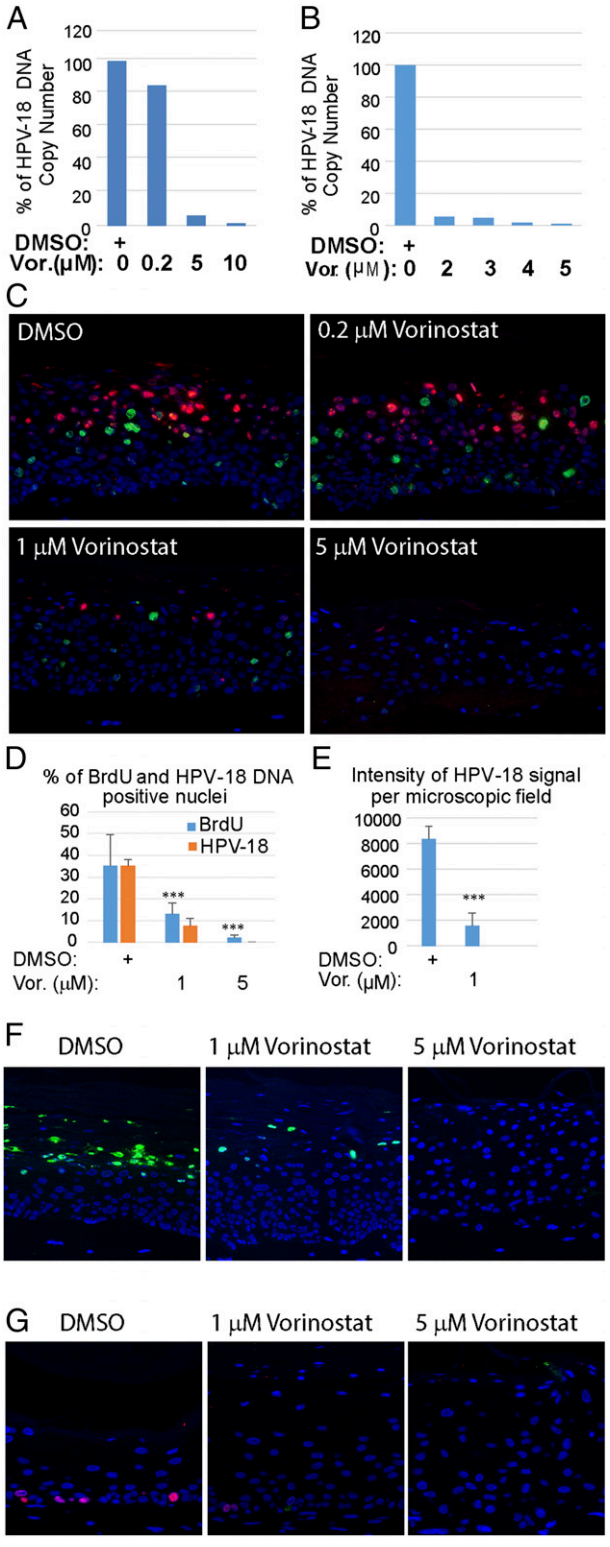

Fig. 2. Effects of Vorinostat on HPV-18 DNA amplification and cellular DNA synthesis. Relative HPV-18 DNA copy number/cell was computed from qPCR of total DNA, extracted from fresh day 13 raft cultures following exposure (*A*) to DMSO (as 100%) (0) or 0.2 (0.2), 5 (5), or 10 μM (10) of Vorinostat, or (*B*) to DMSO (0), 2 (2), 3 (3), 4 (4), or 5 (5) μM Vorinostat from days 6 to 13. (*C*) In situ detection of HPV-18 DNA (red/cy3) and BrdU incorporation (green/FitC) in FFPE tissue sections of HPV-18 raft cultures exposed to DMSO or Vorinostat. Nuclei were detected with DAPI. (*D*) Average percentage of BrdU-positive and HPV-18–positive nuclei from four nonoverlapping microscopic fields per slide from the above experiment (*C*: DMSO, 1 or 5 μM Vorinostat) using the Count And Measure Application of cellSens software (Olympus). (*E*) Average intensity of HPV-18 DNA signals from the same microscopic fields as in *D*. Error bars in *D* and *E* represent SD. (*F*) Indirect IF detection of the major capsid protein L1 (green) in day 14 HPV-18 raft cultures treated with DMSO or Vorinostat from days 6 to 14. (*G*) Indirect IF probing for BrdU incorporation (red) in day 13 uninfected cultures exposed to DMSO or to Vorinostat from days 6 to 13. ***$P < 0.001$.

possibly because of a difference from differentiating squamous epithelium.

Reduction of E7-Induced Nbs1, MRE11, and Activated ATM. Because E7 induces a DDR, which is essential to support HPV DNA amplification (6, 7), we next performed systematic analyses to investigate how proteins in the DDR pathways might be affected in HPV-infected cultures exposed to Vorinostat. E7 activates ATM by increasing phospho-ATM S1981 (3, 6, 7). Consistent with previous reports, IB showed that HPV-18 infection elevated total and phospho-ATM relative to uninfected PHK raft cultures. They also revealed that Vorinostat reduced phospho-ATM (S1981) in HPV-18 raft cultures treated at 1 μM concentrations, while the total ATM level was not affected. However, at 5 μM, neither total nor phosphorylated ATM was detectable (Fig. 5*D*).

The MRN complex (Mre11/Rad50/Nbs1) is a sensor of double-stranded DNA breaks, and it recruits ATM to the sites of damage. The complex prevents the accumulation of DNA damage by promoting restart of a stalled replication fork (39). The MRN complex also initiates ATM/ATR-dependent homologous DNA recombination in S phase and G2 phase in normal and in stressed cells, thereby improving the prospect for cell survival (40). IB analyses confirmed that both Nbs1 and Mre11 proteins were elevated in HPV-18 raft cultures relative to normal PHK raft cultures (Fig. 5 *D* and *E*), in agreement with the previous report that HPV-31 increases Nbs1 to support its replication (41). In the presence of 5 μM Vorinostat, the levels of both proteins decreased. In particular, Nbs1 was reduced to the level of the uninfected PHK raft culture (Fig. 5*D*). The decrease in these DDR proteins is consistent with diminished E7 activity and could have also contributed to the dramatic reduction in viral DNA amplification. We anticipated that it would also increase host DNA damage when chromatin replication forks are halted (see *Induction of γ-H2AX in Infected Cultures*).

Cleavage of DNA-Dependent Protein Kinase Catalytic Subunit. We next examined the steady-state level of DNA-dependent protein kinase catalytic subunit (DNA-PKcs). This protein regulates the nonhomologous end-joining (NHEJ) pathway and is activated by ATM- and ATR-mediated phosphorylation in response to cellular replication stress (42). Even though HPV DNA amplification is unlikely to use NHEJ, compromised NHEJ would exacerbate host DNA damage and enhance apoptosis in the differentiated infected cells (see *Induction of Apoptosis in HPV-18–Infected Cultures*).

Antibody specific for the activated, phosphorylated DNA-PKcs (S2056) is known to detect a slow-migrating band greater than the 260-kDa marker, which likely represents the full-length protein (460 kDa). It also detected several faster-migrating bands of ∼240, 150, and 120 kDa in molecular mass. During apoptosis, the slow-migrating phosphorylated DNA-PKcs band is lost while fast-migrating fragments increase, as caspase 3 cleaves DNA-PKcs (43). In two independent experiments (designated a and b in Fig. 5*F*), the total DNA-PKcs and the full-length phosphorylated DNA-PKcs (S2056) were highly elevated in vehicle-treated or 0.2 μM Vorinostat-treated cultures relative to the uninfected PHK raft culture. Both decreased in 1 μM and 5 μM Vorinostat-treated cultures (Fig. 5*F*, *Upper*), whereas two fast-migrating bands significantly increased (Fig. 5*F*, *Lower*). One band migrated slower than the 140-kDa marker, while the

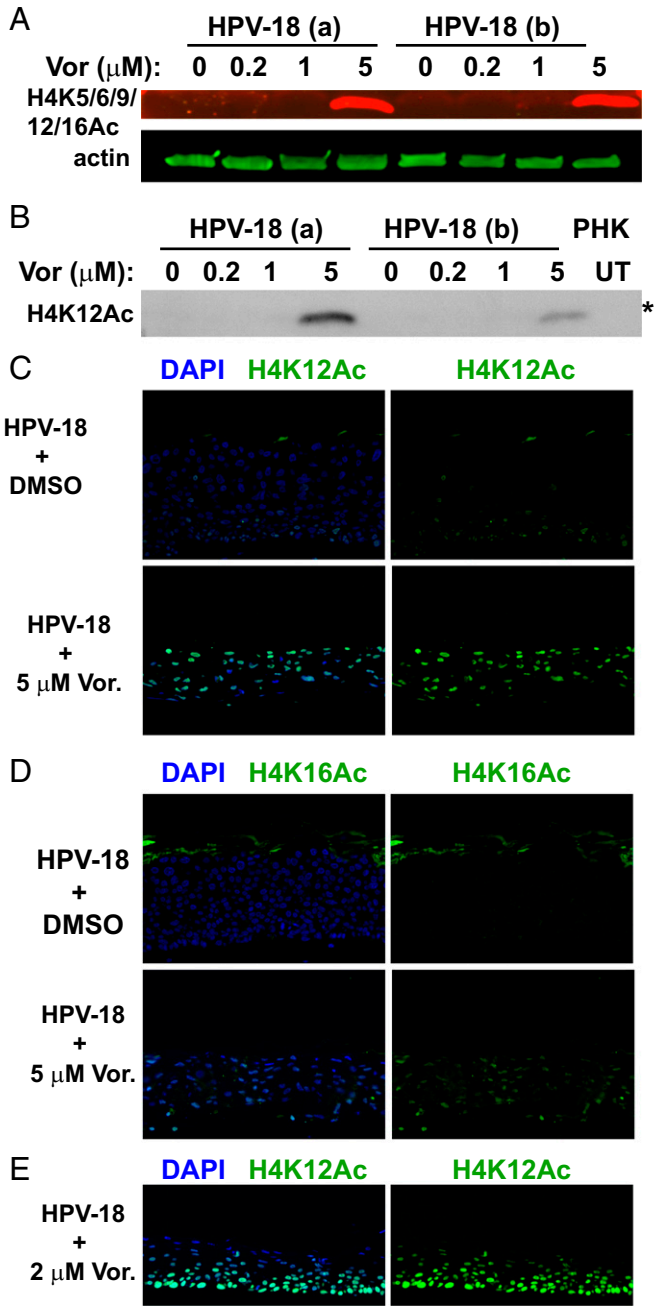

Fig. 3. Detection of acetylated histone 4 in the presence or absence of Vorinostat. (*A*) Acetylated histone 4 was detected with antibody reactive to H4 K5/6/9/12/16 (red signals) in IBs of lysates from two independent sets of day 13 HPV-18–infected cultures (*a* and *b*). The cultures were exposed to DMSO (0) or to 0.2, 1, or 5 μM Vorinostat from days 6 to 13. Acetylated H4 (n red) and actin (in green) were recorded with the LI-COR CLx system. (*B*) Acetylated H4K12 was detected in the IB of the above lysates using the enhanced chemiluminescence (ECL) method. Lysate from UT PHK was one of the controls. This IB (marked with an asterisk) was derived from the same gel as depicted for HDAC-2 in Fig. 4*A* and for HDAC-5 and actin loading reference in Fig. 4*B*. Indirect IF detection of elevated (*C*) H4K12Ac and (*D*) H4K16Ac in day 13 HPV-18 raft cultures in the DMSO-treated control (*Upper*) or exposed to 5 μM Vorinostat (*Lower*) from days 6 to 13. (*E*) Indirect IF detection of H4K12Ac (green) in day 13 HPV-18 raft cultures treated with 2 μM Vorinostat from days 6 to 13. In *C*–*E*, merged images are shown in which nuclei were detected with DAPI and acetylated H4K in green (*Left*), while only the acetylated H4K signals were shown (*Right*).

other more prominent band migrated slower than the 95-kDa marker. These results are indicative of apoptosis in the infected cultures treated with Vorinostat.

Induction of γ-H2AX in Infected Cultures. The Vorinostat inhibition of replicating chromatin remodeling along with down-regulated DDR would lead to accumulation of DNA damage. Using indirect IF, we examined the levels of γ-H2AX (S139), a biomarker of double-stranded DNA breaks. Signals were evident in a subset of cells in the differentiated strata of HPV-18 raft cultures treated with Vorinostat at 5 μM (Fig. 6*A*). In contrast, Vorinostat induced little or no γ-H2AX in uninfected PHK raft cultures (Fig. 6*B*, *Lower*). IBs detected a weak or strong γ-H2AX (S139) band in HPV-18 raft cultures exposed to 1 or 5 μM

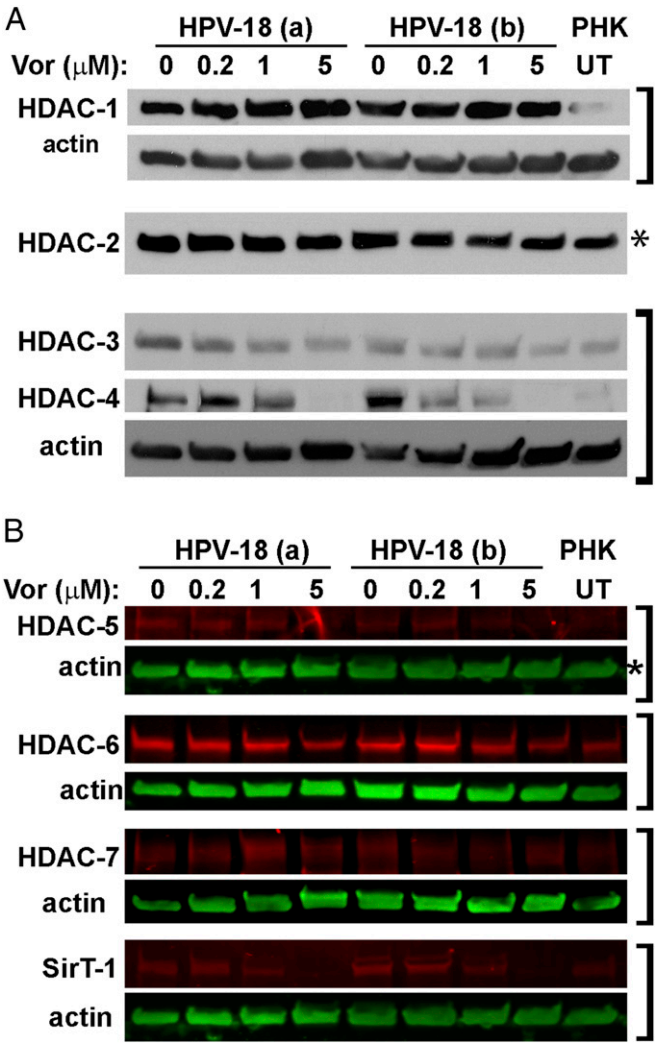

Fig. 4. IBs to detect HDACs in control and Vorinostat-treated day 13 raft cultures. (*A*) IBs of lysates of HPV-18 and PHK raft cultures reveal steady-state levels of HDAC-1, HDAC-2, HDAC-3, and HDAC-4. The cultures were exposed to vehicle (0) or Vorinostat at three concentrations, as indicated, from days 6 to 13. Lysates from UT PHK raft cultures served as one of the controls. The signals were detected with ECL. (*B*) HDACs-5, HDAC -6, HDAC -7, and SirT-1 (in red) and actin (in green) from the same raft cultures were documented with the LI-COR CLx system. Brackets indicate blots from the same gel. Panels showing bands for H4K12Ac in Fig. 3*B* as well as bands of HDAC2 in *A* and HDAC5 in *B* (each marked with an asterisk) were detected in strips from the same gel.

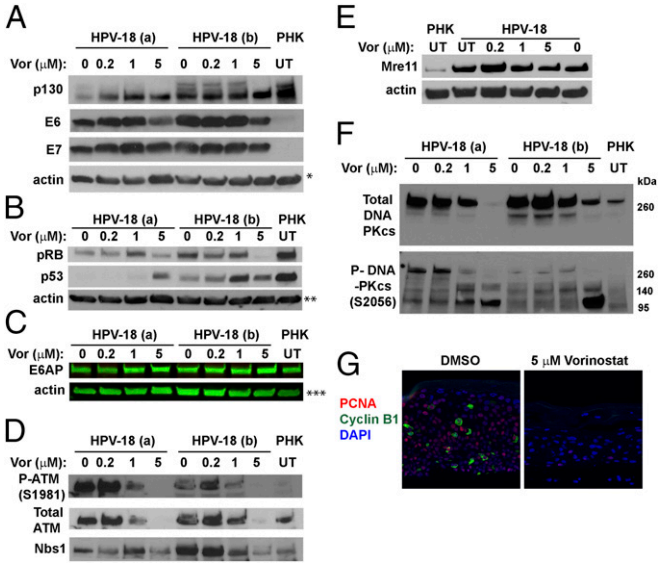

Fig. 5. IBs and IF to detect steady-state levels of HPV-18 E6 and E7 and target host proteins. (*A* and *B*) Two sets of independent day 13 HPV-18 cultures were exposed to the indicated Vorinostat concentrations from days 6 to 13. UT PHK or HPV-18–infected raft cultures exposed to vehicle (0) served as references. Actin was loading control. The ECL detection system was used to detect (*A*) p130, HPV-18 E6 and E7, and actin, (*B*) pRB, p53, and actin, (*D*) total ATM, phosphorylated ATM S1981, and Nbs1, (*E*) Mre-11 and actin, and (*F*) total (*Upper*) and phosphorylated (*Lower*) DNA-PKcs. (*C*) E6AP and actin were detected and documented with LI-COR CLx system. Images in *A*–*C* and *E* each represent blots from a separate gel. Protein bands identified in *D* and *F* are from the same gel as those in *A* and *B*, respectively. (*G*) PCNA (red) and cyclin B1 (green) were detected by IF in FFPE sections from one set of the infected cultures, exposed to DMSO (*Left*) or 5 μM Vorinostat (*Right*). *A* and *F* are from the same gel and had same actin loading control, indicated by a single asterisk (*) in *A*. ** and *** indicate actin loading controls of *B* and *C* IBs.

Vorinostat (Fig. 6*C*), whereas no signal was detected in UT PHK raft cultures, nor in UT or vehicle-treated HPV-18 raft cultures.

Induction of Apoptosis in HPV-18–Infected Cultures. In HPV-18 raft cultures exposed to 5 μM Vorinostat, the histological changes and induction of γ-H2AX, as well as the loss of the full-length phosphorylated DNA-PKcs accompanied by the appearance of degraded short forms, together are suggestive of the occurrence of apoptosis. To substantiate this interpretation, we examined the cultures for the presence of cleaved caspase 3, a marker for early-stage commitment toward apoptosis. It was only detected in HPV-18 cultures treated with 5 μM Vorinostat (Fig. 6*A*). The in situ observation was confirmed by IB (Fig. 6*E*). We then performed terminal deoxynucleotidyl transferase dUTP nick end labeling (TUNEL) assays to probe for extensive DNA fragmentation (Fig. 6*B*, *Upper*). In vehicle-treated HPV-18 raft cultures, only occasional terminally differentiated uppermost cells were positive for a low-intensity TUNEL signal, attributable to normal programmed cell death. At 1 μM of Vorinostat, more TUNEL signals were observed, primarily in the superficial cells and in desquamated tissues (see additional discussion below). At 5 μM of Vorinostat, about 33% of suprabasal cells (averaged over several microscopic fields) accumulated high nuclear TUNEL signals, confirming DNA breakage and apoptosis occurring in these spinous cells (Fig. 6*B*, *Upper* and Fig. 6*D*).

Histology and the indirect IF of uninfected raft cultures revealed that Vorinostat at 1 and 5 μg/mL did not undergo terminal differentiation (Fig. 1*B*). TUNEL signals were detected mostly in desquamated cells, not in the live epithelium (Fig. 6*B*, *Lower*). We suggest that the upper strata of the treated cultures underwent premature programmed cell death without complete degradation of the cellular DNA. The residual DNA was then detected by the TUNEL assay. Even at 5 μM, the cultures exhibited very few TUNEL-positive nuclei (2 to 3%) in the living tissue (Fig. 6*B*, *Lower* and Fig. 6*D*). Collectively, these results suggest that HPV-18–infected cultures were substantially more sensitive than uninfected PHK raft cultures to Vorinostat-caused DNA damage and associated apoptosis.

To determine whether more effective cell killing can be achieved without increasing the Vorinostat concentration, we treated HPV-18 raft cultures with 1 or 5 μM Vorinostat from day 6 through day 22. This prolonged exposure to the higher concentration led to extensive cytopathic effects throughout the epithelium (Fig. 7). The tissue became hypertrophic, and there was no clear demarcation between dead and live tissues. Some suprabasal cells accumulated DNA damage as indicated by γ-H2AX incorporation. Furthermore, DAPI staining revealed a continuous basal layer, but there was significant void in suprabasal strata, suggestive of loss of apoptosed cells. Premature programmed cell death occurred, as virtually all of the desquamated cells retained their nucleus and were γ-H2AX– and TUNEL-positive.

Induction of the Proapoptotic Bim-L and Bim-S. To investigate the apoptotic pathway in these tissue cultures, we used IBs to evaluate the p53-induced proapoptotic proteins Bax, PUMA, NOXA, and Apaf1 (9), as might be expected from an elevated p53 in Vorinostat-treated cultures. However, relative to the vehicle-treated control, Apaf1, PUMA, and Bax were all reduced at 5 μM Vorinostat exposure, where apoptosis occurred (Fig. 8*A*). Thus, stabilized p53 did not appear to be transcriptionally active and responsible for apoptosis observed in HPV-18 raft cultures.

HPV E7 destabilizes pocket proteins and activates E2F1-3 transcription factors (4, 44). Prolonged exposure of cervical cancer

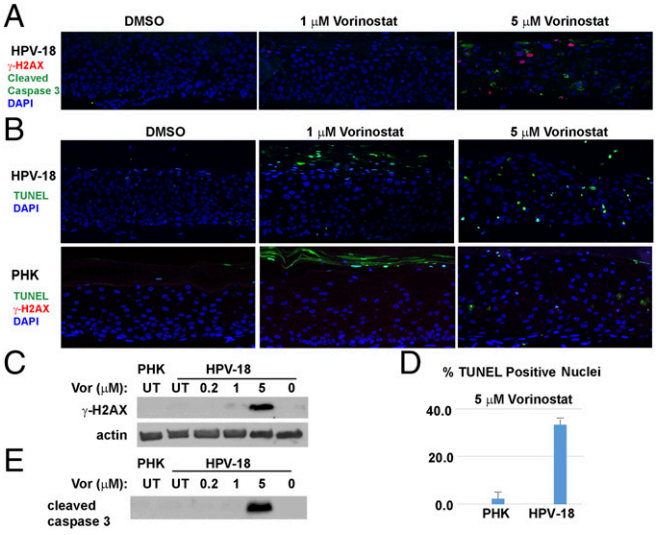

Fig. 6. Assays to detect DNA damage and apoptosis in day 13 PHK and HPV-18–infected raft cultures. (*A*) Detection of cleaved caspase 3 (green) and γ-H2AX (S139) (red) in HPV-18 raft cultures following exposure to DMSO or Vorinostat (1 and 5 μM) from days 6 to 13. (*B*) HPV-18 raft cultures were probed for TUNEL (green) (*Upper*), whereas PHK raft cultures were probed for TUNEL (green) and γ-H2AX (red) (*Lower*). (*C*) IB detection of γ-H2AX S139 in parallel HPV-18 raft cultures. Lysates from UT PHK or infected raft culture as well as infected culture exposed to vehicle (0) were used as references. Actin served as a loading control. (*D*) Percentage of TUNEL-positive nuclei in *A* and *B* were averaged from four microscopic fields under a 20× objective. (*E*) IB detection of cleaved caspase 3 in parallel Vorinostat-treated HPV-18 raft and untreated PHK raft cultures. This strip of IB was derived from the same gel as depicted in Fig. 5*E*, and the actin loading control was presented in Fig. 5*E*.

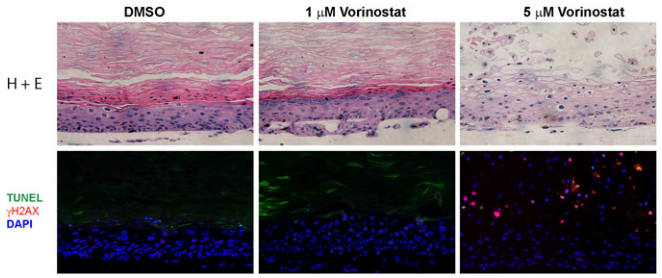

Fig. 7. Prolonged exposure of HPV-18–infected raft culture to Vorinostat. The day 22 cultures were exposed to DMSO or 1 or 5 μM Vorinostat from days 6 to 22. Histology was revealed by staining with hematoxylin and eosin (*Upper*). DNA damage and apoptosis were detected by indirect immunofluorescent detection of γ-H2AX and TUNEL (*Lower*).

cells to Vorinostat leads to E2F1-mediated apoptosis (45). E2F1 up-regulates EZH2, a component of the PRC2 transcription repressor complex (46), which contains the HDAC corepressors (47). EZH2 expression is elevated in proliferating cells and cancers, while it is reduced in differentiated cells (48, 49). The proapoptotic Bim protein is also up-regulated by E2F-1 (50), but it is under the negative control of the PRC2/HDAC repressor complex (51). Thus, depletion of EZH2 and inhibition of HDACs with Vorinostat decrease the activity of EZH2 while elevating Bim, thereby reducing cell proliferation and inducing apoptosis in human cancer cell lines with elevated E2F-1 (52).

Three alternatively spliced isoforms of Bim called Bim-EL, Bim-L, and Bim-S are detected in mammalian cells. They are BH3-only proapoptotic members of the Bcl2 family. Cytotoxicity of the Bim isoforms is inversely related to their size, with the shortest (Bim-S) being the most potent mediator of apoptosis (53). The EZH2–Bim axis is a target of virus infection. For example, Bim expression is repressed by EZH2 in Epstein–Barr virus infections (54). EZH2 is elevated by HPV E7 protein in cultured cells as well as in high-grade dysplasias and cervical cancers, while its depletion inhibited proliferation of E7-expressing keratinocytes in submerged cultures (55). In raft cultures expressing HPV-18 E6 and E7 oncogenes, EZH2 RNA was up-regulated (56). However, the role of EZH2 has not been investigated in productive HPV infections.

Accordingly, we examined EZH2 and Bim expression by IBs to determine whether they play a role in the apoptosis observed in the Vorinostat-treated HPV-infected cultures. EZH2 protein was slightly higher in HPV-18 raft cultures relative to the PHK raft cultures. This level was reduced to that present in uninfected cultures in the presence of Vorinostat (Fig. 8*B*, *Upper*). In contrast, the effects of Vorinostat on the activity EZH2 were evident by examining its target gene Bim (Fig. 8*B*, *Lower*). Relative to PHK raft cultures, a slow-migrating band representing Bim-EL was elevated in UT and vehicle-treated HPV-18 raft cultures. This band intensity was not affected by exposure to 0.2 and 1 μM Vorinostat. However, at 5 μM Vorinostat, levels of this protein and especially two faster-migrating bands, possibly corresponding to alternatively spliced forms Bim-L and Bim-S, were highly elevated. Elevated Bim expression was confirmed by indirect IF in the tissue sections (Fig. 8*C*).

A number of other mechanisms for elevated induction or alternative splicing of Bim have been described (52). In particular, HDAC-3 and HDAC-4 repress Bim expression in non-small cell lung cancer and multiple myeloma cell lines through non-EZH2–dependent mechanisms (57, 58). Thus, reduced levels of HDAC-3 and HDAC-4 in 5 μM Vorinostat-treated HPV-18 raft cultures (Fig. 4*A*) offer additional mechanisms for elevated expression of Bim isoforms. Collectively, the above observations strongly suggest that Vorinostat at 5 μM promotes the Bim-mediated apoptotic pathways in HPV-18 raft cultures.

Effects of Vorinostat on Raft Cultures Containing Other HPV Types. So far, we have described inhibitory effects of Vorinostat on host and HPV-18 proteins. It is reasonable to propose that similar effects would be observed in raft cultures harboring and expressing genomes or oncogenes of other HPV genotypes. Because of the lack of model system to support the productive program of the LR HPV-6 or HPV-11, we conducted a surrogate experiment. Raft cultures were prepared from PHKs acutely transduced with a retrovirus expressing the HPV-11 E7 protein. While HPV-11 E7 alone is able to promote S-phase reentry in suprabasal cells, it does so rather ineffectively relative to HPV-18 E7 (5, 59). We selected an E7 G22D mutant form which has a slightly increased efficiency (60). In this experiment, very few suprabasal cells were positive for BrdU incorporation. Nevertheless, upon exposure to 1 μg/mL of Vorinostat from days 7 to 14, BrdU signal incorporation was entirely abolished. At 5 μg/mL, toxicity was obvious, as tissue was very thin, with no morphologically distinct strata. The γ-H2AX signals

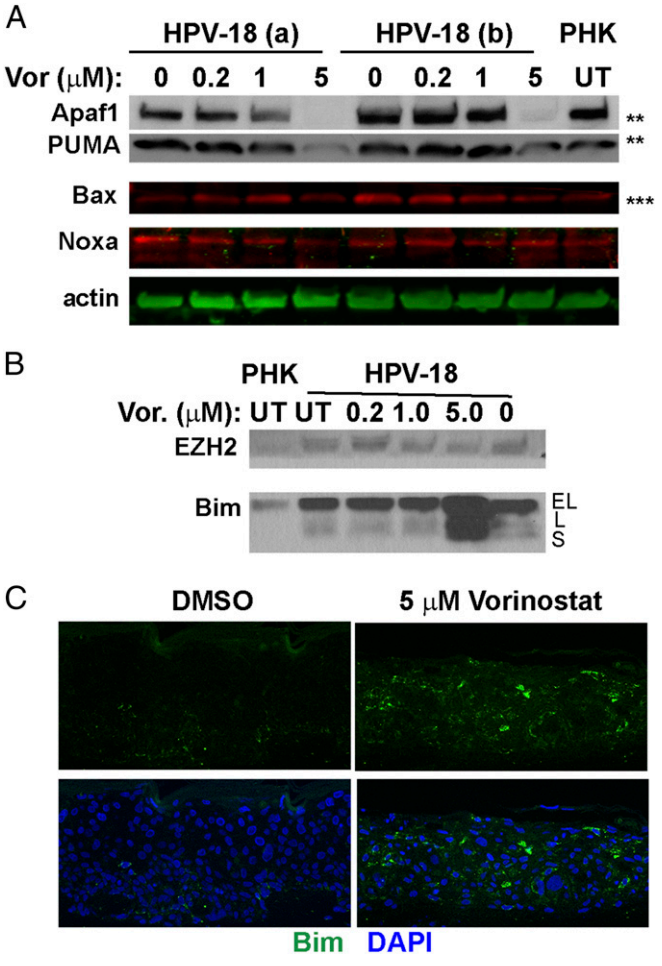

Fig. 8. IBs and IF to detect steady-state levels of the proapoptotic proteins. (*A*) Apaf1, PUMA, Bax, and Noxa. IBs marked with ** and *** are from the same gels as shown in Fig. 5 *B* and *C*, which included the actin loading control. (*B*) IBs to detect EZH2 (*Upper*) and Bim (*Lower*) in day 13 lysates from UT PHK and HPV-18 cultures as well as HPV-18 raft cultures exposed to Vorinostat from days 6 to 13 at the indicated concentrations. EL, L, and S indicate extralong, long, and small forms of Bim, respectively. The blots are from the same gels as presented in Figs. 5*E* and 6*C*, where the actin loading controls are shown. (*C*) Indirect IF detection of Bim protein (green) in tissue sections of HPV-18 raft cultures.

were detected in live tissue whereas TUNEL was observed in the superficial layer, possibly because the few spinous cells that reentered S phase were already lost to apoptosis (*SI Appendix*, Fig. S2). We infer that Vorinostat would also be effective in inhibiting LR HPV DNA amplification.

Next, we examined raft cultures of an immortalized cell line W12-E which harbor extrachromosomal HPV-16 genomic plasmids (61). The cells were subcloned from W12 cells established from a cervical dysplasia (62). UT W12-E cells formed a stratified squamous epithelium (Fig. 9*A*, *Upper Left*). Unexpectedly, not only did BrdU incorporation completely cease in the presence of 1 μg/mL Vorinostat, but extensive cell death was evident (*Upper Middle*). At 5 μg/mL, all cells in the tissue died (Fig. 9*A*, *Upper Right*). The induction of γ-H2AX and TUNEL signals supported these conclusions (Fig. 9*A*, *Lower*). These results suggest that immortalized cells appear more sensitive to Vorinostat than primary cells.

To evaluate whether cells transformed by HPV are also similarly sensitive to Vorinostat, we tested raft cultures of CaSki cells, a cell line derived from a cervical cancer. CaSki cells harbor about 600 copies of the integrated HPV-16 genome and express the E6 and E7 genes (63, 64). The CaSki cell raft culture formed a highly dysplastic tissue which was composed entirely of undifferentiated cells with some apoptosis already occurring (Fig. 9*B*). The raft cultures were indeed highly sensitive to Vorinostat. At 1 μg/mL, the majority of the cells underwent apoptosis, as judged by TUNEL assay. At 5 μg/mL, only remnant dead tissue remained.

The Inhibitory Effects of Belinostat and Panobinostat. Belinostat (65) and Panobinostat (66) are new HDAC inhibitors approved by the Food and Drug Administration for clinical applications against peripheral T-cell lymphoma and resistant multiple myeloma. To rule out the possibility that the inhibition observed with Vorinostat was due to an off-target effect, we performed side-by-side comparisons of Vorinostat, Belinostat, and Panobinostat in HPV-18–infected cultures. Based on published reports, a range of concentrations were tested. The cultures were exposed to the inhibitors from day 6 to day 14, harvested on day 14, and examined for histology and probed with DNA-FISH and indirect IF (Fig. 10 and *SI Appendix*, Figs. S3 and S4).

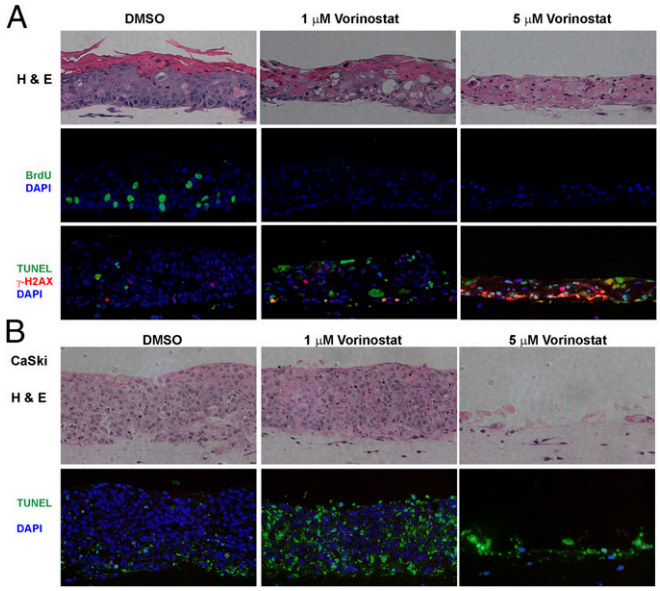

Fig. 9. Effects of Vorinostat on raft cultures of W12-E cells (*A*) and CaSki cells (*B*). Day 14 cultures were exposed to DMSO (*Left*) or 1 (*Middle*) or 5 μM (*Right*) Vorinostat from days (*A*) 6 to 14 or (*B*) 5 to 14. Rows are as follows: (*A*) histology (*Upper*), BrdU incorporation (*Middle*), and γ-H2AX and TUNEL (*Lower*) signals; (*B*) histology (*Upper*) and TUNEL (*Lower*) signals.

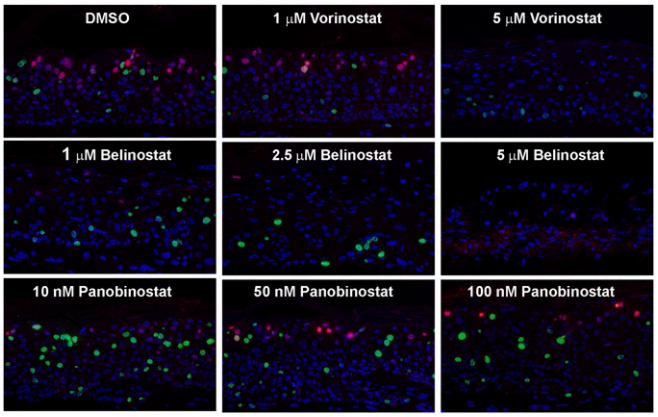

Fig. 10. HPV-18–infected raft cultures exposed to Vorinostat, Belinostat, or Panobinostat. Parallel cultures were exposed to these HDAC inhibitors at the specified concentration from days 6 to 14. Day 14 cultures were probed for viral DNA amplification (red) and BrdU incorporation (green). Portions of the cultures exposed to 5 μM Belinostat had significant cell death, causing trapping of in situ probe signals (red). Histology, L1, and TUNEL assays are shown in *SI Appendix*, Figs. S3 and S4.

Belinostat had a stronger inhibitory effect on viral DNA amplification relative to that of Vorinostat (Fig. 10, *Upper* and *Middle* rows). As expected, it abrogated L1 expression (*SI Appendix*, Fig. S3*B*). Belinostat killed the infected raft culture more effectively than Vorinostat, as evident from histology. A partial disintegration of the cultures was observed at 5 μg/mL of Belinostat (*SI Appendix*, Fig. S3*A*, compare cultures treated with 5 μM Belinostat or 5 μM Vorinostat). In agreement, at 5 μM, Belinostat induced much more extensive γ-H2AX and TUNEL signals than Vorinostat (compare *SI Appendix*, Fig. S4 to Fig. 6 *A* and *B*). Up to 100 nM, Panobinostat exhibited no morphologically visible toxicity in the infected culture (*SI Appendix*, Fig. S3*A*). It only reduced viral DNA amplification slightly but did not abrogate host DNA replication (Fig. 10, *Lower* row). Consequently, it did not abolish viral L1 expression (*SI Appendix*, Fig. S3*B*). At 250 nM, apoptosis began to appear, and, at 1 μM, Panobinostat caused extensive DNA damage and cell death (*SI Appendix*, Fig. S4). Taken together, these results suggest that the inhibitory effects observed with Vorinostat are shared with at least one other HDAC inhibitor, affirming our conclusion that HDACs are the main targets. However, the possibility of additional dysregulated pathways cannot be ruled out.

Discussion

Histone acetylation by HATs and deacetylation by HDACs play critical roles in nucleosome remodeling, in regulating gene expression, and in fork progression of replicating chromatinized DNA (32). Vorinostat is known to sensitize cancer cells in vitro and tumors in xenografts to apoptosis by DNA damage-inducing agents. This is the basis for using HDAC inhibitors in cancer therapeutics. Because HPV induces S-phase reentry in differentiated cells, host cell DNA replication and viral DNA amplification in these cells should be subject to the same regulation by HDACs. In this study, we applied the pan-HDAC inhibitor Vorinostat as a single agent to determine whether perturbation of HDAC activities would influence viral DNA amplification and cell survival in epithelial tissue cultures developed from PHKs, an organotypic system which provides a physiologically relevant environment.

We found that Vorinostat at 0.2 μM has nondiscernable effect on tissue histology and minimal effects on host DNA replication and viral DNA amplification. Of note, this treatment increased the levels of certain host and viral proteins including E6, E7,

ATM, phospho-ATM, and Mre11. One interpretation is that this low concentration of Vorinostat promoted open chromatin and increased transcription. In contrast, exposure from days 6 through 13 to higher Vorinostat concentrations, host DNA replication, and viral DNA amplification were dramatically inhibited. More than 30% of the cells underwent apoptosis after this short treatment (Fig. 6). Prolonged exposure from days 6 through 22 induced widespread toxicity (Fig. 7). With different effectiveness, an 8-d exposure to two other pan-HDAC inhibitors, Belinostat and Panobinostat, also inhibited viral DNA amplification or cellular DNA replication (Fig. 10). As expected, higher concentrations led to more cell death (*SI Appendix*, Figs. S3 and S4).

Detailed in situ analyses and biochemical interrogation of Vorinostat-treated cultures suggest several causes for these effects. First, the HDAC inhibitor halts suprabasal cellular DNA replication, reducing progression to G2 phase during which viral DNA amplifies. Second, viral DNA replication forks may also stall, resulting in degradation and loss. Third, the activities of viral oncoproteins are compromised, stabilizing the underphosphorylated form of p130, the increase of which could reduce S-phase reentry. Fourth, DDR proteins were down-regulated, further hampering viral DNA amplification. Lastly, with stalled host chromatin replication and compromised DDR, DNA damage accumulates, leading to apoptosis. In this respect, the end results are similar to treatment with octadecycloxyethyl benzyl phosphonyl methoxyethyl guanine (ODE-Bn-PMEG), an acyclic nucleoside phosphonate prodrug and obligate chain terminator when incorporated into DNA. Exposure of HPV-18–infected raft cultures to ODE-Bn-PMEG leads to extensive DNA damage and apoptosis and possible loss of HPV genomes in remaining cells (67).

The exposure to Vorinostat led to stabilized p53. However, the p53 protein was transcriptionally inactive, as it did not elevate p53-responsive, proapoptotic proteins such *as BAX*, *PUMA*, *Apaf1*, and *Noxa* (Fig. 8*A*). Rather, these proteins were reduced. We previously reported on raft cultures infected with HPV-18 E6 mutants incapable of destabilizing p53. Despite high levels of p53 in numerous cells, there was no apoptosis in these cultures, indicative of transcriptionally inactive p53 (3, 11). Our data show that apoptosis is mediated by proapoptotic Bim isoforms (Fig. 8), known to be up-regulated by E2F-1 and a primary cause of death in Vorinostat-treated cancer cells (50, 68).

How does exposure to 1 or 5 μM Vorinostat compromise the abilities of E6 and E7 to destabilize p130 and p53 (Fig. 5 *A* and *B*)? The activity and stability of p53 are tightly regulated by alternative posttranslational acetylation or ubiquitination on its many lysine residues. The acetylated lysine residues must be deacetylated for polyubiquitination and degradation to occur (69, 70). The loss of their activities could explain why p53 became elevated in Vorinostat-treated raft cultures. The elevated p53 could also have contributed to the inability to amplify viral DNA (4, 11). Similarly, Vorinostat could have reduced or prevented polyubiquitination of p130, thereby stabilizing it. The elevated hypophosphorylated p130 would then contribute to the severe reduction in S-phase cells. At 5 μM Vorinostat, a very low level of pRB was detected despite the compromised E7 activity (Fig. 5*B*). We suggest several possible explanations. First, p300-mediated acetylation of the lysine residues in the C-terminal domain of hypophosphorylated pRB increases its association with MDM2, a ubiquitin ligase (71). MDM2 can destabilize pRB, but not 130, in a ubiqitination-independent manner (72). Second, Vorinostat may have caused the basal cells to exit the cell cycle and become quiescent, and quiescent cells have low pRB but high p130. This possibility is supported by the complete loss of BrdU incorporation and cytoplasmic cyclin B1 accumulation (indicative of prolonged G2 phase) from treated raft cultures (Fig. 2*C* and Fig. 5*G*, *Right*). In concordance, the E7-induced proliferating cell nuclear antigen (PCNA), a processivity factor for DNA poly δ, was only infrequently detected (Fig. 5*G*, *Right*). In contrast, in the control DMSO-exposed HPV-18 raft cultures, BrdU incorporation (Fig. 2*C*), cytoplasmic cyclin B1, and nuclear PCNA were observed in basal and suprabasal cells (Fig. 5*G*, *Left*), as described previously (3, 7, 67). Thus, most of the cells in treated HPV-18 raft cultures had indeed exited the cell cycle.

Although E6 and E7 activities were compromised by 1 or 5 μM Vorinostat, the E6 and E7 protein levels were not significantly reduced relative to UT cultures. We speculate that E6 and E7 might normally be degraded in a complex with their respective target proteins. Thus, when p53 and p130 remained acetylated and could not be destabilized by the viral proteins, the viral proteins were also stabilized. This hypothesis is consistent with the observation that more-potent E7 proteins are shorter lived than less active E7 in raft cultures (60).

Because one of the major mechanisms of action by HDAC inhibitors is their interference in chromatin replication, the inhibitory effect is not expected to restrict to HPV-18 cultures. Indeed, Vorinostat prevents BrdU incorporation in raft cultures expressing the LR HPV-11 E7 alone (*SI Appendix*, Fig. S2). In one case report, Vorinostat stabilized HPV-11–associated lung tumors after a yearlong treatment (73). We have now shed some light on the mechanisms involved. Importantly, we also show that raft cultures of HPV-16 immortalized W12-E cells derived from a cervical dysplasia and HPV-16 transformed CaSki cells derived from a cervical cancer were highly sensitive to Vorinostat, triggering widespread apoptosis at as low as 1 μM exposure. We speculate that these cell lines are already deficient in elements in DDR pathways, further sensitizing them to HDAC inhibitors. Our results suggest that HDAC inhibitors could also be useful in treating cervical dysplasias or possibly cancers, perhaps in combination with other DNA damaging agents currently used in the clinic.

In conclusion, our experiments revealed that HPV-18 infection induces S-phase reentry in differentiated cells and elevates protein levels of multiple HDACs. HDAC inhibitor Vorinostat reduces viral oncoprotein activities, and it also inhibits and down-regulates the expression of a number HDACs that are necessary for remodeling the replicating chromatin. As a result, HPV DNA amplification and host DNA replication are abrogated. Importantly, HPV infection sensitizes the cells to Vorinostat, which selectively induces DNA damage and apoptosis in HPV-infected raft cultures relative to uninfected cells. On the basis of these observations, we suggest that HDAC inhibitors are promising compounds for treating benign HPV infections, abrogating progeny production, and hence interrupting infectious transmission. It remains to be further investigated whether they might also be useful in treating HPV associated dysplasias and cancers.

ACKNOWLEDGMENTS. We thank Dr. Paul Lambert for sharing W12-E cells and Prof. Hengbin Wang, PhD, for sharing antibodies against EZH2. We acknowledge the Department of Cell, Developmental and Integrative Biology, University of Alabama at Birmingham (UAB) for the use of their LI-COR CLx documentation system. We are indebted to the nurses in the UAB Well-Baby Nursery for collecting neonatal foreskins from elective circumcisions. This research was supported by National Institutes of Health Grant CA83679 and by funds from the Anderson Family Endowed Chair (to L.T.C.), by the UAB Comprehensive Cancer Center/HIV-Associated Malignancy Pilot Grant 316851 and Comprehensive Cancer Center of UAB Pilot Grant 5P30CA013148-43, and by UAB Bridge Funding (to N.S.B.) (2017–2018).

1. de Martel C, Plummer M, Vignat J, Franceschi S (2017) Worldwide burden of cancer attributable to HPV by site, country and HPV type. *Int J Cancer* 141:664–670.
2. Stoler MH, Wolinsky SM, Whitbeck A, Broker TR, Chow LT (1989) Differentiation-linked human papillomavirus types 6 and 11 transcription in genital condylomata revealed by in situ hybridization with message-specific RNA probes. *Virology* 172:331–340.
3. Wang HK, Duffy AA, Broker TR, Chow LT (2009) Robust production and passaging of infectious HPV in squamous epithelium of primary human keratinocytes. *Genes Dev* 23:181–194.
4. McLaughlin-Drubin ME, Münger K (2009) The human papillomavirus E7 oncoprotein. *Virology* 384:335–344.

5. Genovese NJ, Banerjee NS, Broker TR, Chow LT (2008) Casein kinase II motif-dependent phosphorylation of human papillomavirus E7 protein promotes p130 degradation and S-phase induction in differentiated human keratinocytes. *J Virol* 82:4862–4873.
6. Moody CA, Laimins LA (2009) Human papillomaviruses activate the ATM DNA damage pathway for viral genome amplification upon differentiation. *PLoS Pathog* 5:e1000605.
7. Banerjee NS, Wang HK, Broker TR, Chow LT (2011) Human papillomavirus (HPV) E7 induces prolonged G2 following S phase reentry in differentiated human keratinocytes. *J Biol Chem* 286:15473–15482.
8. McKinney CC, Hussmann KL, McBride AA (2015) The role of the DNA damage response throughout the papillomavirus life cycle. *Viruses* 7:2450–2469.
9. Matt S, Hofmann TG (2016) The DNA damage-induced cell death response: A roadmap to kill cancer cells. *Cell Mol Life Sci* 73:2829–2850.
10. Howie HL, Katzenellenbogen RA, Galloway DA (2009) Papillomavirus E6 proteins. *Virology* 384:324–334.
11. Kho EY, Wang HK, Banerjee NS, Broker TR, Chow LT (2013) HPV-18 E6 mutants reveal p53 modulation of viral DNA amplification in organotypic cultures. *Proc Natl Acad Sci USA* 110:7542–7549.
12. Struhl K (1998) Histone acetylation and transcriptional regulatory mechanisms. *Genes Dev* 12:599–606.
13. Haberland M, Montgomery RL, Olson EN (2009) The many roles of histone deacetylases in development and physiology: Implications for disease and therapy. *Nat Rev Genet* 10:32–42.
14. Li Y, Shin D, Kwon SH (2013) Histone deacetylase 6 plays a role as a distinct regulator of diverse cellular processes. *FEBS J* 280:775–793.
15. Saunders LR, Verdin E (2007) Sirtuins: Critical regulators at the crossroads between cancer and aging. *Oncogene* 26:5489–5504.
16. Telles E, Seto E (2012) Modulation of cell cycle regulators by HDACs. *Front Biosci (Schol Ed)* 4:831–839.
17. Chakraborty S, et al. (2014) Nuclear matrix protein SMAR1 represses c-Fos-mediated HPV18 E6 transcription through alteration of chromatin histone deacetylation. *J Biol Chem* 289:29074–29085.
18. Zhao W, et al. (1999) Trichostatin A up-regulates human papillomavirus type 11 upstream regulatory region-E6 promoter activity in undifferentiated primary human keratinocytes. *J Virol* 73:5026–5033.
19. Smith JA, et al. (2014) SMCX and components of the TIP60 complex contribute to E2 regulation of the HPV E6/E7 promoter. *Virology* 468–470:311–321.
20. Jha S, et al. (2010) Destabilization of TIP60 by human papillomavirus E6 results in attenuation of TIP60-dependent transcriptional regulation and apoptotic pathway. *Mol Cell* 38:700–711.
21. Thomas MC, Chiang CM (2005) E6 oncoprotein represses p53-dependent gene activation via inhibition of protein acetylation independently of inducing p53 degradation. *Mol Cell* 17:251–264.
22. Ferreira R, Magnaghi-Jaulin L, Robin P, Harel-Bellan A, Trouche D (1998) The three members of the pocket proteins family share the ability to repress E2F activity through recruitment of a histone deacetylase. *Proc Natl Acad Sci USA* 95:10493–10498.
23. Longworth MS, Wilson R, Laimins LA (2005) HPV31 E7 facilitates replication by activating E2F2 transcription through its interaction with HDACs. *EMBO J* 24:1821–1830.
24. Wong S, Weber JD (2007) Deacetylation of the retinoblastoma tumour suppressor protein by SIRT1. *Biochem J* 407:451–460.
25. Luo J, et al. (2001) Negative control of p53 by Sir2alpha promotes cell survival under stress. *Cell* 107:137–148.
26. Vaziri H, et al. (2001) hSIR2(SIRT1) functions as an NAD-dependent p53 deacetylase. *Cell* 107:149–159.
27. Allison SJ, Jiang M, Milner J (2009) Oncogenic viral protein HPV E7 up-regulates the SIRT1 longevity protein in human cervical cancer cells. *Aging (Albany NY)* 1:316–327.
28. Wang C, et al. (2006) Interactions between E2F1 and SirT1 regulate apoptotic response to DNA damage. *Nat Cell Biol* 8:1025–1031.
29. Langsfeld ES, Bodily JM, Laimins LA (2015) The deacetylase Sirtuin 1 regulates human papillomavirus replication by modulating histone acetylation and recruitment of DNA damage factors NBS1 and Rad51 to viral genomes. *PLoS Pathog* 11:e1005181.
30. Das D, Smith N, Wang X, Morgan IM (2017) The deacetylase SIRT1 regulates the replication properties of human papillomavirus 16 E1 and E2. *J Virol* 91:e00102-17.
31. Bhaskara S (2015) Histone deacetylases 1 and 2 regulate DNA replication and DNA repair: Potential targets for genome stability-mechanism-based therapeutics for a subset of cancers. *Cell Cycle* 14:1779–1785.
32. Stengel KR, Hiebert SW (2015) Class I HDACs affect DNA replication, repair, and chromatin structure: Implications for cancer therapy. *Antioxid Redox Signal* 23:51–65.
33. Lin Z, et al. (2009) Combination of proteasome and HDAC inhibitors for uterine cervical cancer treatment. *Clin Cancer Res* 15:570–577.
34. Cheng S, Schmidt-Grimminger DC, Murant T, Broker TR, Chow LT (1995) Differentiation-dependent up-regulation of the human papillomavirus E7 gene reactivates cellular DNA replication in suprabasal differentiated keratinocytes. *Genes Dev* 9:2335–2349.
35. Sirbu BM, Cortez D (2013) DNA damage response: Three levels of DNA repair regulation. *Cold Spring Harb Perspect Biol* 5:a012724.
36. Ou YH, Chung PH, Sun TP, Shieh SY (2005) p53 C-terminal phosphorylation by CHK1 and CHK2 participates in the regulation of DNA-damage-induced C-terminal acetylation. *Mol Biol Cell* 16:1684–1695.
37. Scheffner M, Huibregtse JM, Vierstra RD, Howley PM (1993) The HPV-16 E6 and E6-AP complex functions as a ubiquitin-protein ligase in the ubiquitination of p53. *Cell* 75:495–505.
38. Kao WH, Beaudenon SL, Talis AL, Huibregtse JM, Howley PM (2000) Human papillomavirus type 16 E6 induces self-ubiquitination of the E6AP ubiquitin-protein ligase. *J Virol* 74:6408–6417.
39. Trenz K, Smith E, Smith S, Costanzo V (2006) ATM and ATR promote Mre11 dependent restart of collapsed replication forks and prevent accumulation of DNA breaks. *EMBO J* 25:1764–1774.
40. Lavin MF, Kozlov S, Gatei M, Kijas AW (2015) ATM-dependent phosphorylation of all three members of the MRN complex: From sensor to adaptor. *Biomolecules* 5:2877–2902.
41. Anacker DC, Gautam D, Gillespie KA, Chappell WH, Moody CA (2014) Productive replication of human papillomavirus 31 requires DNA repair factor Nbs1. *J Virol* 88:8528–8544.
42. Davis AJ, Chen BPC, Chen DJ (2014) DNA-PK: A dynamic enzyme in a versatile DSB repair pathway. *DNA Repair (Amst)* 17:21–29.
43. Song Q, et al. (1996) DNA-dependent protein kinase catalytic subunit: A target for an ICE-like protease in apoptosis. *EMBO J* 15:3238–3246.
44. Johnson BA, Aloor HL, Moody CA (2017) The Rb binding domain of HPV31 E7 is required to maintain high levels of DNA repair factors in infected cells. *Virology* 500:22–34.
45. Finzer P, et al. (2002) Growth arrest of HPV-positive cells after histone deacetylase inhibition is independent of E6/E7 oncogene expression. *Virology* 304:265–273.
46. Kuzmichev A, Jenuwein T, Tempst P, Reinberg D (2004) Different EZH2-containing complexes target methylation of histone H1 or nucleosomal histone H3. *Mol Cell* 14:183–193.
47. van der Vlag J, Otte AP (1999) Transcriptional repression mediated by the human polycomb-group protein EED involves histone deacetylation. *Nat Genet* 23:474–478.
48. Gall Trošelj K, Novak Kujundzic R, Ugarkovic D (2016) Polycomb repressive complex's evolutionary conserved function: The role of EZH2 status and cellular background. *Clin Epigenetics* 8:55.
49. Ezhkova E, et al. (2009) Ezh2 orchestrates gene expression for the stepwise differentiation of tissue-specific stem cells. *Cell* 136:1122–1135.
50. Zhao Y, et al. (2005) Inhibitors of histone deacetylases target the Rb-E2F1 pathway for apoptosis induction through activation of proapoptotic protein Bim. *Proc Natl Acad Sci USA* 102:16090–16095.
51. Wu ZL, et al. (2010) Polycomb protein EZH2 regulates E2F1-dependent apoptosis through epigenetically modulating Bim expression. *Cell Death Differ* 17:801–810.
52. Sionov RV, Vlahopoulos SA, Granot Z (2015) Regulation of Bim in health and disease. *Oncotarget* 6:23058–23134.
53. O'Connor L, et al. (1998) Bim: A novel member of the Bcl-2 family that promotes apoptosis. *EMBO J* 17:384–395.
54. Wood CD, et al. (2016) MYC activation and BCL2L11 silencing by a tumour virus through the large-scale reconfiguration of enhancer-promoter hubs. *eLife* 5:e18270.
55. Holland D, et al. (2008) Activation of the enhancer of zeste homologue 2 gene by the human papillomavirus E7 oncoprotein. *Cancer Res* 68:9964–9972.
56. Garner-Hamrick PA, et al. (2004) Global effects of human papillomavirus type 18 E6/E7 in an organotypic keratinocyte culture system. *J Virol* 78:9041–9050.
57. Tanimoto A, et al. (2017) Histone deacetylase 3 inhibition overcomes *BIM* deletion polymorphism-mediated osimertinib resistance in *EGFR*-mutant lung cancer. *Clin Cancer Res* 23:3139–3149.
58. Vallabhapurapu SD, et al. (2015) Transcriptional repression by the HDAC4-RelB-p52 complex regulates multiple myeloma survival and growth. *Nat Commun* 6:8428.
59. Banerjee NS, et al. (2006) Conditionally activated E7 proteins of high-risk and low-risk human papillomaviruses induce S phase in postmitotic, differentiated human keratinocytes. *J Virol* 80:6517–6524.
60. Genovese NJ, Broker TR, Chow LT (2011) Nonconserved lysine residues attenuate the biological function of the low-risk human papillomavirus E7 protein. *J Virol* 85:5546–5554.
61. Jeon S, Allen-Hoffmann BL, Lambert PF (1995) Integration of human papillomavirus type 16 into the human genome correlates with a selective growth advantage of cells. *J Virol* 69:2989–2997.
62. Sterling J, Stanley M, Gatward G, Minson T (1990) Production of human papillomavirus type 16 virions in a keratinocyte cell line. *J Virol* 64:6305–6307.
63. Baker CC, et al. (1987) Structural and transcriptional analysis of human papillomavirus type 16 sequences in cervical carcinoma cell lines. *J Virol* 61:962–971.
64. Van Tine BA, et al. (2004) Clonal selection for transcriptionally active viral oncogenes during progression to cancer. *J Virol* 78:11172–11186.
65. Thompson CA (2014) Belinostat approved for use in treating rare lymphoma. *Am J Health Syst Pharm* 71:1328.
66. Ocio EM, et al. (2010) In vitro and in vivo rationale for the triple combination of panobinostat (LBH589) and dexamethasone with either bortezomib or lenalidomide in multiple myeloma. *Haematologica* 95:794–803.
67. Banerjee NS, Wang HK, Beadle JR, Hostetler KY, Chow LT (2018) Evaluation of ODE-Bn-PMEG, an acyclic nucleoside phosphonate prodrug, as an antiviral against productive HPV infection in 3D organotypic epithelial cultures. *Antiviral Res* 150:164–173.
68. Lindemann RK, et al. (2007) Analysis of the apoptotic and therapeutic activities of histone deacetylase inhibitors by using a mouse model of B cell lymphoma. *Proc Natl Acad Sci USA* 104:8071–8076.
69. Li M, Luo J, Brooks CL, Gu W (2002) Acetylation of p53 inhibits its ubiquitination by Mdm2. *J Biol Chem* 277:50607–50611.
70. Gu W, Roeder RG (1997) Activation of p53 sequence-specific DNA binding by acetylation of the p53 C-terminal domain. *Cell* 90:595–606.
71. Chan HM, Krstic-Demonacos M, Smith L, Demonacos C, La Thangue NB (2001) Acetylation control of the retinoblastoma tumour-suppressor protein. *Nat Cell Biol* 3:667–674.
72. Sdek P, et al. (2005) MDM2 promotes proteasome-dependent ubiquitin-independent degradation of retinoblastoma protein. *Mol Cell* 20:699–708.
73. Yuan H, et al. (2012) Use of reprogrammed cells to identify therapy for respiratory papillomatosis. *N Engl J Med* 367:1220–1227.